European Journal of Medicinal Chemistry 50 (2012) 280–287

Contents lists available at SciVerse ScienceDirect

European Journal of Medicinal Chemistry

journal homepage: http://www.elsevier.com/locate/ejmech

Original article

Synthesis and photodynamic properties of adamantylethoxy Zn(II) phthalocyanine derivatives in different media and in human red blood cells

A. Laura Ochoa, Tomas C. Tempesti, Mariana B. Spesia, M. Elisa Milanesio, Edgardo N. Durantini*

Departamento de Química, Facultad de Ciencias Exactas Físico-Químicas y Naturales, Universidad Nacional de Río Cuarto, Agencia Postal Nro. 3, X5804BYA Río Cuarto, Córdoba, Argentina

ARTICLE INFO

Article history:
Received 7 October 2011
Received in revised form
2 February 2012
Accepted 3 February 2012
Available online 10 February 2012

Keywords:
Synthesis
Zinc(II) phthalocyanine
Adamantane
Photodynamic properties
Human red blood

ABSTRACT

Novel unsymmetrically substituted Zn(II) phthalocyanine bearing an adamantylethoxy group (AZnPc) was synthesized by the ring expansion reaction of boron(III) subphthalocyanine chloride with an appropriated phthalonitrile derivative (APc). Also, APc was used to obtain a new Zn(II) phthalocyanine bearing four adamantylethoxy groups (A_4ZnPc) by cyclotetramerization reaction. The spectroscopic and photodynamic properties of these photosensitizers were compared with those of a Zn(II) phthalocyanine substituted by four methoxy groups (M_4ZnPc) in different media. Similar results were obtained in *N*,*N*-dimethylformamide. However, a higher photodynamic activity was found for AZnPc in a biomimetic system formed by reverse micelles. This behavior was also observed in the presence of human red blood (HRB) cells, which were used as an *in vitro* cellular model. Thus, AZnPc was the most effective photosensitizer to produce HRB cells hemolysis. The photodynamic effect produced a decrease in the HRB cells osmotic stability leading to the release of hemoglobin. Studies of photodynamic action mechanism showed that photohemolysis of HRB cells was protected in the presence of azide ion, while the addition of mannitol produced a negligible effect on the cellular photodamage, indicating the intermediacy of $O_2(^1\Delta_g)$. Therefore, the presence of an adamantyl unit in the phthalocyanine macrocycle represents an interesting molecular architecture for potential phototherapeutic agents.

1. Introduction

Phthalocyanine derivatives have attracted a considerable amount of attention as second-generation of phototherapeutic agents for the treatment of malignant tumors by photodynamic therapy (PDT) [1,2]. These photosensitizers generally have larger extinction coefficients in the therapeutically convenient 650–800 nm range and appropriated photochemical properties [3]. To date, a great variety of symmetrically substituted phthalocyanines have been extensively studied. The intrinsic symmetry of the phthalocyanines sometimes represents a limitation for many purposes. In contrast, unsymmetrically substituted phthalocyanines offer a possibility of improving selectivity since groups with different properties may be attached to the ring. Thus, the chance of designing and synthesizing unsymmetrical compounds with substituents located at specific positions may facilitate enhanced applications of phthalocyanines [4]. The design of A_3B-phthalocyanines bearing one different (B) and three identical (A) isoindole subunits can be used to incorporate a biological active structure covalently linked to the macrocycle. Different strategies have been employed for the preparation of these A_3B-symmetry derivatives. However, the most efficient selective approach involves ring expansion reaction of subphthalocyanines using a substituted phthalonitrile [4–7].

Adequate photosensitizers for PDT should have specific chemical and biological properties [8]. Two of the photochemical requisites are a high absorption coefficient in the visible region of the spectrum and a long lifetime of triplet excited state to produce efficiently reactive oxygen species (ROS). In this approach visible light is used to active a photosensitizer, which can react with molecules from its direct environment by electron or hydrogen transfer, leading to the production of radicals (type I reaction), or it can transfer its energy to oxygen, generating the highly reactive singlet molecular oxygen, $O_2(^1\Delta_g)$ (type II reaction). Both mechanisms can occur simultaneously and the ratio between the two processes is influenced by the sensitizer, substrate and the nature of the microenvironment [9].

In biological media, cell membranes seem to be important targets for many antineoplastic photosensitizer agents. In this sense, mammalian erythrocytes serve as convenient model cells for exploration of physiological and molecular mechanisms involved in

* Corresponding author. Tel.: +54 358 4676157; fax: +54 358 4676233.
E-mail address: edurantini@exa.unrc.edu.ar (E.N. Durantini).

0223-5234/$ – see front matter © 2012 Elsevier Masson SAS. All rights reserved.
doi:10.1016/j.ejmech.2012.02.005

PDT [10]. Red blood cells have been often used for *in vitro* PDT studies [11–16]. Though erythrocytes are not ideal cells to evaluate or quantitatively compare photosensitizers, they are useful to elucidate the cellular and molecular principles of PDT [17].

In this paper, novel Zn(II) phthalocyanine derivatives substituted by one (AZnPc) or four (A_4ZnPc) adamantylethoxy groups were synthesized. In previous studies, Zn(II) phthalocyanines substituted with four adamantane moieties were synthesized from the corresponding phthalonitriles. However, *in vitro* photodynamic activity using adamantyl phthalocyanines has not yet been reported [18,19]. Adamantane is a highly lipophilic compound, which has been used to modify the biological availability of several molecules. Among the major biological activities displayed by adamantane derivatives, the antiviral, antibacterial, antifungal, anti-inflammatory are the most important ones [20,21]. The value of the adamantyl group in drug design has been recognized most recently in agents to treat iron overload disease, malaria and type 2 diabetes [22]. Also, in the present work, the spectroscopic and photodynamic characteristics of AZnPc and A_4ZnPc were studied in a homogeneous medium and in reverse micelles. The results obtained for these new adamantylethoxy phthalocyanines were compared with those of Zn(II) 2,9,16,23-tetrakis(methoxy)phthalocyanine (M_4ZnPc), which is an active photosensitizer for potential use in PDT [23–25]. Photodynamic action was then evaluated *in vitro* using human red blood (HRB) cells under different conditions to obtain information about the effect produced by these phthalocyanines.

2. Materials and methods

2.1. General

Absorption and fluorescence spectra were recorded on a Shimadzu UV-2401PC spectrometer (Shimadzu Corporation, Tokyo, Japan) and on a Spex FluoroMax spectrofluorometer (Horiba Jobin Yvon Inc, Edison, NJ, USA), respectively. Proton nuclear magnetic resonance spectra were recorded on an FT-NMR Bruker Advance 200 (Rheinstetten, Germany) at 200 MHz and on an FT-NMR Bruker Avance DPX400 spectrometer at 400 MHz. Mass Spectra were taken with a Bruker micrO-TOF-QII (Bruker Daltonics, MA, USA) equipment with an ESI source operated in positive/negative mode, using nitrogen as nebulizing and drying gas and sodium formiate (10 mM) as internal calibrant. IR spectra were recorded on a Bruker Tensor 27 FT-IR (Ettlingen, Germany). The visible light source used to irradiate erythrocytes was a Novamat 130 AF (Braun Photo Technik, Nürnberg, Germany) slide projector equipped with a 150 W lamp. The light was filtered through a 2.5 cm glass cuvette filled with water to absorb heat. A wavelength range between 350 and 800 nm was selected by optical filters. The light intensity at the treatment site was 300 W/m^2 (Radiometer Laser Mate-Q, Coherent, Santa Clara, CA, USA).

All the chemicals from Aldrich (Milwaukee, WI, USA) were used without further purification. Silica gel thin-layer chromatography (TLC) plates 250 microns from Analtech (Newark, DE, USA) were used. Solvents (GR grade) from Merck (Darmstadt, Germany) were distilled. Ultrapure water was obtained from a Labconco (Kansas, MO, USA) equipment model 90901-01.

2.2. Synthesis of phthalocyanines

Zn(II) 2,9,16,23-tetrakis(methoxy)phthalocyanine (M_4ZnPc) was synthesized as previously described [23].

2.2.1. 4-[2-(1-Adamantyl)ethoxy]phthalonitrile (APn)

A mixture of 4-nitrophthalonitrile (90 mg, 0.52 mmol), 2-(1-adamantyl)ethanol (97 mg, 0.54 mmol) and *t*-BuOK (65 mg, 0.58 mmol) in 5 mL of DMSO was stirred for 20 min at room temperature under argon atmosphere. Then, the mixture was treated with water (20 mL) and extracted with dichloromethane (two portions of 20 mL each). The solvent was removed under reduced pressure. The product was purified by flash chromatography column (silica gel, dichloromethane/*n*-heptane 30%) yielding 113 mg (72%) of the pure phthalonitrile APn. TLC (silica gel) R_f (dichloromethane/*n*-heptane 50%) = 0.30. ^{1}HNMR ($CDCl_3$, TMS) δ [ppm] 1.48 (t, 2H, CH_2CH_2O, J = 6.0 Hz), 1.52 (br, s, 6H, CH_2), 1.68 (br, s, 6H, CH_2), 1.98 (bs, s, 3H, bridgehead, CH), 4.10 (t, 2H, CH_2O, J = 6.0 Hz), 7.17 (dd, 1H, J = 2.6 Hz, 9.0 Hz), 7.25 (d, 1H), 7.69 (d, 1H, J = 9.0 Hz). EI-MS [m/z] 306 (M^+) (306.1732 calculated for $C_{20}H_{22}N_2O$). FT-IR (KBr) cm^{-1} 2916, 2848, 2232 (CN), 1596, 1450, 1344, 1325, 1289, 1255, 1087, 1011, 873, 835. Anal. calcd. C 78.40, H 7.24, N 9.14, found C 78.34, H 7.29, N 9.09.

2.2.2. Zn(II) 2-[2-(1-adamantyl)ethoxy]phthalocyanine (AZnPc)

A solution of APn (13 mg, 0.042 mmol) and 1,8-diazabicyclo [5.4.0]undec-7-ene (DBU) (8 μL, 0.08 mmol) in DMSO (2 mL) was heated to 130 °C under an argon atmosphere. Then, a suspension of boron(III) subphthalocyanine chloride (SubPc, 43 mg, 0.10 mmol) and Zn(II) acetate dihydrate (30 mg, 0.14 mmol) in DMSO/1-chloronaphthalene (2 mL, 2:1) was added drop-wise to the heated mixture over a period of 1 h. The reaction was kept at 130–140 °C for 24 h. The reaction mixture was cooled to room temperature and precipitated with cool water (25 mL). The solid was separated by centrifugation and the product was purified by flash chromatography column (silica gel, dichloromethane/*n*-heptane 10%) yielding 10 mg (15%) of the pure AZnPc. TLC (silica gel) R_f (dichloromethane/*n*-heptane 10%) = 0.10. ^{1}HNMR ($CDCl_3$, TMS) δ [ppm] 1.50–1.80 (m, 14H, CH_2CH_2O and adamantanyl CH_2), 1.98 (bs, s, 3H, bridgehead, CH), 4.25 (t, 2H, CH_2O, J = 6.0 Hz), 7.30–8.00 (m, 15H). ESI-MS [m/z] 755.2225 $(M + H)^+$ (754.2147 calculated for $C_{44}H_{34}N_8OZn$). FT-IR (KBr) cm^{-1} 2922, 2850, 1602, 1454, 1331, 1279, 1089, 1057, 879, 750. Anal. calcd. C 69.89, H 4.53, N 14.82, found C 69.97, H 4.46, N 14.89. Absorption spectrum λ_{max} (DMF) [nm] (log ε) 343 (4.95), 604 (4.53), 668 (5.29).

2.2.3. Zn(II) 2,9(10),16(17),23(24)-tetrakis[2-(1-adamantyl)ethoxy] phthalocyanine (A_4ZnPc)

A solution of APn (20 mg, 0.065 mmol) and Zn(II) acetate dihydrate (11 mg, 0.05 mmol) in 2 mL of *n*-pentanol was stirred for 10 min under argon atmosphere. Then, DBU (10 μL, 0.10 mmol) was added and the mixture was refluxed for 15 h. The reaction mixture was cooled at room temperature and precipitated with methanol (25 mL). The solid was filtered and washed with water to yield 6 mg (27%) of A_4ZnPc. TLC (silica gel) R_f (dichloromethane/*n*-heptane 10%) = 0.78. ^{1}HNMR ($CDCl_3$, TMS) δ [ppm] 1.50–1.80 (m, 56H, CH_2CH_2O and adamantyl CH_2), 1.99 (bs, s, 12H, bridgehead, CH), 4.10–4.20 (m, 8H, CH_2O), 7.30–8.00 (m, 12H). ESI-MS [m/z] 1323.5909 $(M + Cl)^-$ (negative mode) (1288.6220 calculated for $C_{80}H_{88}N_8O_4Zn$). FT-IR (KBr) cm^{-1} 2920, 2848, 1605, 1447, 1329, 1277, 1093, 1049, 876, 747. Anal. calcd. C 74.43, H 6.87, N 8.68, found C 74.38, H 6.94, N 8.62. Absorption spectrum λ_{max} (DMF) [nm] 352 (4.98), 612 (4.59), 680 (5.31).

2.3. Spectroscopic studies

Absorption and fluorescence spectra were recorded at 25.0 ± 0.5 °C using 1 cm path length quartz cells. The fluorescence quantum yield (Φ_F) of phthalocyanines were calculated by comparison of the area below the corrected emission spectrum in *N*,*N*-dimethylformamide (DMF) with that of Zn(II) phthalocyanine (ZnPc) as a reference (Φ_F = 0.28) [26]. Sample and reference absorbances were matched at the excitation wavelength (610 nm)

and the areas of the emission spectra were integrated in the range 630–800 nm.

2.4. Steady state photolysis

Solutions of 9,10-dimethylanthracene (DMA, 35 μM) and photosensitizer in DMF were irradiated in 1 cm path length quartz cells (2 mL) with monochromatic light at $\lambda_{irr} = 670$ nm (sensitizer absorbance 0.2), from a 75 W high-pressure Xe lamp through a high intensity grating monochromator (Photon Technology Instrument, Birmingham, NJ, USA). The light fluence rate was determined as 15 W/m^2. The kinetics of DMA photooxidation were studied by following the decrease of the absorbance (A) at $\lambda_{max} = 378$ nm. The observed rate constants (k_{obs}) were obtained by a linear least-squares fit of the semilogarithmic plot of Ln A_0/A *vs.* time. Photooxidation of DMA was used to determine $O_2(^1\Delta_g)$ production by the photosensitizers. ZnPc ($\Phi_\Delta = 0.56$) was used as a reference in DMF [27]. Measurements of the sample and reference under the same conditions afforded Φ_Δ for phthalocyanines by direct comparison of the slopes in the linear region of the plots. All the experiment were performed at 25.0 ± 0.5 °C. The pooled standard deviation of the kinetic data, using different prepared samples, was less than 10%.

2.5. Studies in reverse micelles

Studies in reverse micelles were performed using a stock solution of (AOT) 0.1 M, which was prepared by weighing and dilution in *n*-heptane. The addition of water to the corresponding solution was performed using a calibrated microsyringe. The amount of water present in the system was expressed as the molar ratio between water and the AOT present in the reverse micelle ($W_0 = [H_2O]/[AOT]$). In all experiments, $W_0 = 10$ was used. Photosensitized decomposition of DMA was made as explained above in homogenic solution. The values of Φ_Δ were calculated using ZnPc ($\Phi_\Delta = 0.56$) as reference [28].

2.6. Studies in HRB cells

HRB cells were obtained from healthy donors. After extraction, the whole blood was taken into anticoagulant EDTA, centrifuged (3000 rpm for 5 min) to remove plasma and the leukocyte layer, washed three times with phosphate buffer saline (PBS) solution (137 mM NaCl, 2.7 mM KCl, 1.5 mM KH_2PO_4 and 8 mM Na_2HPO_4) and centrifuged again. Erythrocytes were re-suspended in saline solution (0.9% NaCl) to get a concentration of ~10^6 cells/mL and maintained at 4 °C until use [29].

2.7. Photohemolysis assays

The HRB cell suspensions (~10^6 cells/mL) were placed in glass flasks (2 mL) and dark incubated with different concentrations (1–10 μM) of phthalocyanine at room temperature for 30 min. Phthalocyanine was added from a 0.5 mM stock solution in DMF. After incubation HRB cells suspensions were irradiated with visible light as described above. Photosensitized hemolysis was carried out at room temperature. After irradiation, the samples were kept 24 h at room temperature in dark. Then, the tubes were centrifuged and 100 μL of supernatants were diluted in 2 mL of distilled water. The hemoglobin content was determined by measuring the absorbance at 413 nm. Results are expressed as percentage of hemolysis taking 100% as the absorbance obtained from a sample lysed in distilled water [11]. Sodium azide (50 mM) or mannitol (50 mM) were added to HRB cell suspensions from 2.5 M stock solutions in water and the cells were incubated for 30 min at room temperature in dark together with 5 μM phthalocyanine. Then, the samples were treated as described above.

2.8. Osmotic fragility evaluation

Suspensions of HRB cells were treated with 5 μM photosensitizer as described above and irradiated for 3 min with visible light. After that 100 μL of HRB cells suspension were diluted in NaCl solution (2 mL) of various concentrations (0.2–0.9% w/v) buffered with 5 mM sodium phosphate (pH 7.4) [16]. Then, the suspensions were incubated for 24 h at room temperature, centrifuged and the percentage of osmotically lysed cells was estimated [15].

In all studies using HRB cells, control experiments were carried out without illumination in the absence and presence of photosensitizer and irradiating the HRB cells without photosensitizer. Each experiment was repeated separately three times. Variation between groups was evaluated using the Student *t*-test, with a confidence level of 95% ($p < 0.05$) considered statistically significant.

3. Results and discussion

3.1. Synthesis of phthalocyanines derivatives

Two new Zn(II) phthalocyanines substituted by adamantyl units were synthesized from phthalonitrile by a two-step procedure. First, a phthalonitrile derivative (APn) bearing an adamantyl group was prepared by a nucleophilic *ipso*-nitro substitution reaction of 4-nitrophthalonitrile with 2-(1-adamantyl)ethanol in DMSO (Scheme 1). The reaction was carried out in the presence of *t*-BuOK at room temperature. This basic medium was used to activate the nucleophilic capacity of 2-(1-adamantyl)ethanol. The product APn was isolated by flash chromatography with 72% yield. This phthalonitrile derivative was employed to synthesize the AZnPc by ring expansion of SubPc (Scheme 1). The reaction was performed in the presence of DBU and Zn(II) acetate in DMSO/1-chloronaphthalene. After heating the mixture for 24 h, the AZnPc phthalocyanine was purified by flash chromatography with a 15% yield. Under these conditions, only one phthalocyanine was obtained facilitating the purification process. Therefore, this approach has advantages over statistical condensation of two differently substituted phthalonitriles. The latter procedure can results in a complex mixture of products, which difficult the purification process.

On the other hand, the cyclotetramerization of APn with Zn(II) acetate in the presence of organic base DBU was performed in *n*-pentanol (Scheme 1). After reflux for 15 h, the reaction results in the formation of the corresponding A_4ZnPc, which was precipitated with methanol, filtered and washed with water to obtain 27% yield. This method of synthesis produced a mixture of four regioisomers with an adamantyl group at the 2- or 3-positions of each benzene ring in the A_4ZnPc molecule.

Due to the lipophilicity of adamantane, the incorporation of the adamantyl moiety in phthalocyanine macrocycle results in compounds with relatively higher lipophilicity, which in turn can modify the biological availability of these photosensitizers. In AZnPc and A_4ZnPc structures, the adamantyl center is isolated from the phthalocyanine macrocycle by a two carbon aliphatic chain. This spacer provides a higher mobility of the adamantyl moiety, which could facilitate the interaction with the membrane.

3.2. Spectroscopic studies

Absorption spectra of AZnPc and A_4ZnPc were studied in different solvents (Fig. 1). In DMF, both phthalocyanines showed an intense *Q*-bands in the region of ~670 nm, which are characteristic

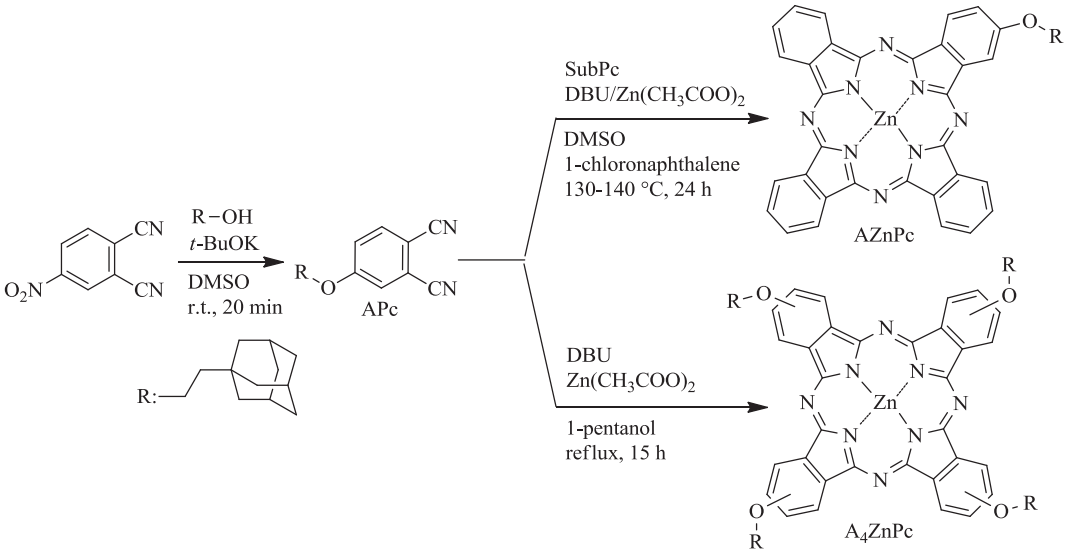

Scheme 1. Synthesis of phthalocyanine derivatives AZnPc and A_4ZnPc.

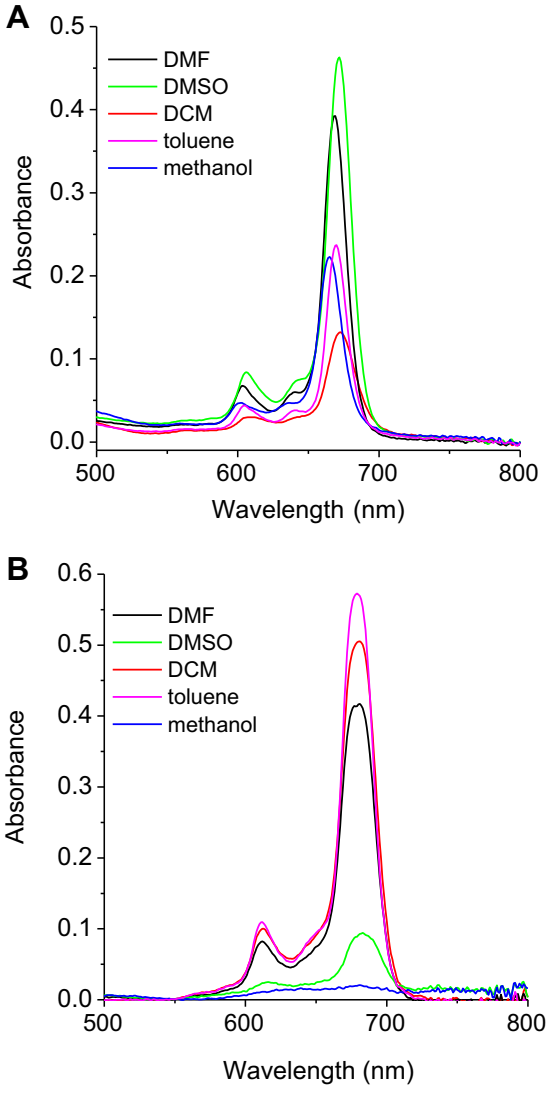

Fig. 1. Absorption spectra of (A) AZnPc and (B) A_4ZnPc in different solvents: *N*,*N*-dimethylformamide (DMF), dimethylsulfoxide (DMSO), dichloromethane (DCM), toluene and methanol; [phthalocyanine] = 2 μM.

of Zn(II) phthalocyanine derivatives dissolved as monomeric molecules [30,31]. Varying the solvent polarity, a small solvatochromic effect is observed on the location of the absorption *Q*-bands. These typical *Q*-bands were also observed for AZnPc in the other organic solvents studied (Fig. 1A). The spectrum of AZnPc in DMSO (Fig. 1A) was as intensive as in DMF at the same concentration. The introduction of four adamantyl substituents in A_4ZnPc was accompanied by an increase in the lipophilic character of the phthalocyanine macrocycle. Thus, A_4ZnPc was better solubilized as monomer in less polar solvents, for example toluene (Fig. 1B). However, A_4ZnPc was very poorly solubilized as monomer in more polar solvents, such as DMSO and methanol, as shown by the broadening and the low intensity of the *Q*-bands (Fig. 1B). Many phthalocyanines have tendency to aggregate in polar solvents especially when the macrocycle is substituted by lipophilic groups [32]. On the other hand, both new adamantyl phthalocyanines are hydrophobic in nature and they were not soluble in pure water.

In Table 1, the spectroscopic properties of AZnPc and A_4ZnPc *Q*-band were compared with that of M_4ZnPc in DMF. The shape and the *Q*-band absorption maximum of AZnPc closely match the spectrum of ZnPc (668 nm) [30]. The *Q*-bands of A_4ZnPc and M_4ZnPc present a ~10 nm bathochromic shift respect to ZnPc due to the auxochromic effect of the four ether groups.

The steady-state fluorescence emission spectra of AZnPc and A_4ZnPc were performed in DMF. As shown in Fig. 2, the spectra showed two bands in the red spectral region, which are characteristic for similar Zn(II) phthalocyanines [3]. As expected from the absorption data, the emission maxima of A_4ZnPc and M_4ZnPc are bathochromically shifted with respect to that of AZnPc. By comparison with ZnPc as a reference, the values of fluorescence quantum yields (Φ_F) were calculated in DMF. The results of Φ_F are summarized in Table 1 and these values are according with previously reported for similar Zn(II) phthalocyanines in solution and

Table 1
Spectroscopic characteristics of phthalocyanines and fluorescence quantum yield (Φ_F) in DMF.

Phthalocyanine	λ_{max} (Abs)[a]	λ_{max} (Emission)	ε (Lmol^{-1} cm^{-1})	Φ_F
AZnPc	668	672	1.96×10^5	0.17 ± 0.02
A_4ZnP	680	688	2.08×10^5	0.25 ± 0.02
M_4ZnP	676	678	2.01×10^5	0.26 ± 0.02

[a] *Q*-band.

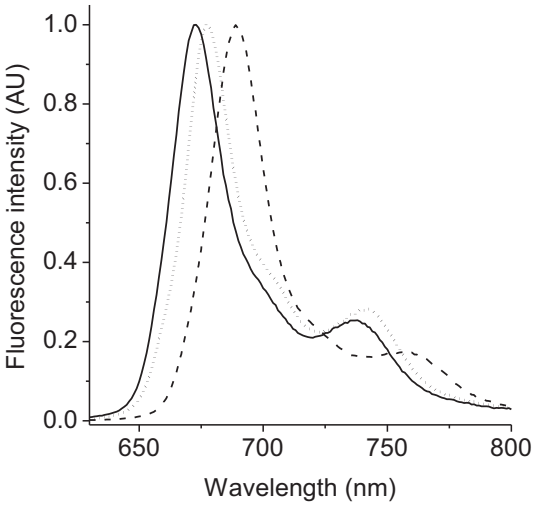

Fig. 2. Normalized fluorescence emission spectra of AZnPc (solid line), A_4ZnPc (dashed line) and M_4ZnPc (dotted line) in DMF; $\lambda_{exc} = 610$ nm.

they are appropriated values for quantification of phthalocyanine by fluorescence emission techniques [23].

3.3. Photodynamic properties

Photooxidation of 9,10-dimethylanthracene (DMA) sensitized by AZnPc and A_4ZnPc phthalocyanines was studied in DMF under aerobic condition (Fig. 3A). Also, the DMA reaction was evaluated in the presence of M_4ZnPc. The values of the observed rate constant (k_{obs}) were calculated from first-order kinetic plots of the DMA absorption at 378 nm *vs*. time (Table 2). In this medium, these phthalocyanines photosensitized the decomposition of DMA with similar rates.

Taking into account that DMA quenches $O_2(^1\Delta_g)$ exclusively by chemical reaction, this substrate can be used as a method to evaluate the ability of the sensitizers to produce $O_2(^1\Delta_g)$ in solution [33]. The quantum yield of $O_2(^1\Delta_g)$ production (Φ_Δ) were calculated comparing the k_{obs} for the corresponding phthalocyanine with that for the reference (ZnPc, $k_{obs} = (1.67 \pm 0.05) \times 10^{-3}$ s^{-1}). Very close values of Φ_Δ were obtained for these phthalocyanines indicating that they are photosensitizers higher efficient to produce $O_2(^1\Delta_g)$ in DMF (Table 2). However, the values of Φ_Δ can significantly change in a different medium, diminishing mainly when the sensitizer is partially aggregated [32]. Also, the photophysics of the phthalocyanines established in solution can be significantly modified in the biological microenvironment where the sensitizer is localized. This limits to predict the photodynamic efficiencies of phthalocyanines in biological systems on the basic of photophysical investigations in homogeneous medium.

Also, photooxidation of DMA sensitized by phthalocyanines under aerobic conditions was performed in *n*-heptane/AOT (0.1 M)/water ($W_0 = 10$). Microheterogeneous systems such as reverse micelles are frequently used as an interesting model to mimic the water pockets that are found in various bioaggregates [34,35]. In reverse micelles, compounds with different polarities can be located in a variety of microenvironments namely the organic surrounded solvent, the water pool or at the micellar interface. Because DMA is a non-polar compound, it is assumed that this substrate is mainly solubilized in the organic pseudophase (*n*-heptane) of the micellar system [34]. In this biomimetic microenvironment, the substrate reacts with the $O_2(^1\Delta_g)$ photosensitized by phthalocyanine. From the plots in Fig. 3B, the values of the k_{obs}

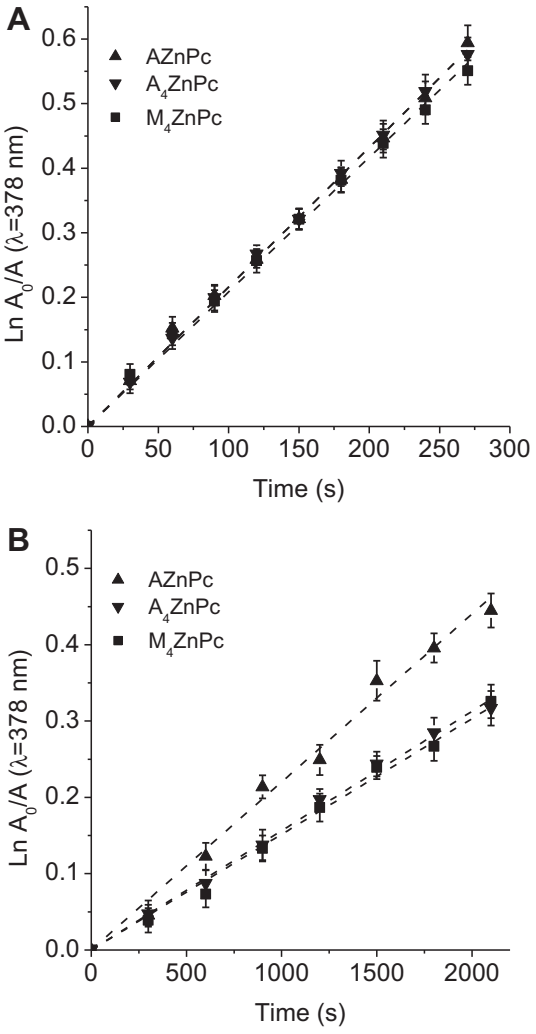

Fig. 3. First-order plots for the photooxidation of DMA photosensitized by AZnPc (▲), A_4ZnPc (▼) and M_4ZnPc (■) in (A) DMF and (B) *n*-heptane/AOT (0.1 M)/water ($W_0 = 10$). Values represent mean ± standard deviation of three separate experiments.

were calculated for DMA reaction in micellar system. As can be observed in Table 2, the value of k_{obs} for AZnPc is higher than those for A_4ZnPc and M_4ZnPc, indicating that AZnPc was the better photosensitizer to decompose DMA in reverse micelles of AOT. Using ZnPc as a reference, the Φ_Δ values were calculated for these phthalocyanines (Table 2). As can be observed, AZnPc was the most efficient photosensitizer to generate $O_2(^1\Delta_g)$ in this microheterogeneous medium. The reason for the monomeric state of these lipophilic phthalocyanines is given by hydrophobic interactions of the photosensitizer with the micelles. In micellar system, phthalocyanines can be located in different microenvironments depending on their structure. In the case of two strong hydrophobic phthalocyanines (AZnPc and A_4ZnPc) the different behavior observed can be due to the asymmetry of AZnPc, which could promote a better location in the micellar interface. The photodynamic activity induced by A_4ZnPc was very similar to that found for M_4ZnPc. Possibly; these symmetrically substituted phthalocyanines are located in the same micellar microenvironment. Thus, photodynamic activity induced by these phthalocyanines in micelles differs from that found in DMF, which is a good solvent for all photosensitizers.

As can be observed in Table 2, the reaction rates of DMA sensitized by these phthalocyanines in DMF are faster than in the AOT

Table 2
Kinetic parameters (k_{obs}) for the photooxidation reaction of DMA and quantum yield of $O_2(^1\Delta_g)$ production (Φ_Δ) of phthalocyanines in different media.

Phthalocyanine	k_{obs}^{DMA} (s^{-1})[a]	Φ_Δ[a]	k_{obs}^{DMA} (s^{-1})[b]	Φ_Δ[b]
AZnPc	$(2.16 \pm 0.08) \times 10^{-3}$	0.72 ± 0.05	$(2.20 \pm 0.08) \times 10^{-4}$	0.75 ± 0.05
A_4ZnP	$(2.16 \pm 0.08) \times 10^{-3}$	0.72 ± 0.05	$(1.59 \pm 0.07) \times 10^{-4}$	0.55 ± 0.05
M_4ZnP	$(2.06 \pm 0.07) \times 10^{-3}$	0.69 ± 0.05	$(1.63 \pm 0.07) \times 10^{-4}$	0.56 ± 0.05

[a] in DMF.
[b] in *n*-heptane/AOT (0.1 M)/water ($W_0 = 10$).

micellar system. Similar behavior was previously observed in AOT reverse micelles using porphyrins as sensitizers [36]. In the AOT micellar system, $O_2(^1\Delta_g)$ is partitioned between the internal and external pseudophases with a partition constant of 0.11 [37]. Consequently, the photooxidation rate of DMA was diminished in the organic pseudophase.

3.4. Photohemolysis of HRB cells

In vitro the photodynamic activity of AZnPc, A_4ZnPc and M_4ZnPc was evaluated by photohemolytic effect on HRB cells. In accordance with cell-culture assays, where cell death is monitored by membrane disruption, hemolysis of red blood cells can be regarded as a mode of measuring death of erythrocytes [10,38]. Hemoglobin absorption spectrum shows an intense *Soret* band at 413 nm and two *Q*-bands at 500–600 nm [39] Thus, spectroscopic measurements of hemoglobin released are much easier and faster to carry out than cell staining and counting. In this way, phthalocyanines are appropriated photosensitizers in presence of blood because they absorb in the phototherapeutic window.

Suspensions of HRB cells ($\sim 10^6$ cells/mL) in saline solution were treated with different concentration of phthalocyanine (1–10 μM) for 30 min at room temperature in dark. In these experiments, the photosensitizers were added from a stock solution (0.5 mM) in DMF because this solvent is soluble in PBS and it can dissolve both phthalocyanines as monomers. Also, control assays using the highest volume of DMF added to the cells (40 μL in 2 mL of cell suspension) showed negligible hemolytic effect on HRB cells. After 24 h without irradiation negligible hemolysis was found indicating no dark toxicity induced by these phthalocyanines. On the other hand, light alone at the highest fluence rate used, did not induce photohemolysis either. Therefore, the hemolysis obtained after irradiation of the erythrocytes cells treated with the phthalocyanine was due to the photosensitization effect of the agent produced by visible light.

The consequent cellular photohemolytic activities produced by each phthalocyanine were compared using 5 μM and different irradiation periods. As can be observed in Fig. 4A, the photohemolysis after HRB irradiation with visible light was dependent upon the phthalocyanine structure and light exposure level. The photohemolysis produced by AZnPc was always higher than M_4ZnPc. After 5 min of irradiation, AZnPc induced a ~75% of cellular lysis, while the phototoxic activity of M_4ZnPc was ~38%. In contrast, this was not the behavior found for the A_4ZnPc, which only induced a ~5% of hemolysis after 30 min irradiation. One of the problems that affect the photosensitizing ability of the phthalocyanines is the aggregation tendency due to the large π conjugate systems [32]. The aggregates present an efficient nonradiative energy relaxation pathway, diminishing the triplet-state population and the $O_2(^1\Delta_g)$ quantum yield. In the present study, the decrease in the photohemolytic activity induced by A_4ZnPc with respect to AZnPc can be due to its higher lipophilic character as result of the four symmetrically distributed adamantyl groups around the macrocycle. It is known that the nature of chemical compounds and their hydrophilic/lipophilic nature strongly affects the dye binding to the cells and, as a consequence, the cytotoxic efficiency [40]. Therefore, the existence of monomers in biological surroundings is important because it allows obtaining a high photosensitizer activity leading to cell damage [41].

Photolytic cellular activities produced by different concentrations of AZnPc (1–10 μM) are shown in Fig. 4B. An increase in the amount of AZnPc from 1 to 5 μM was accompanied by an enhancement in the HRB photodamage. After a short irradiation period of 5 min, the hemolytic effect increased from 13% to 75% for cells treated with 1 and 5 μM, respectively. Under the last condition, complete hemolysis was reached after 30 min of irradiation. Also,

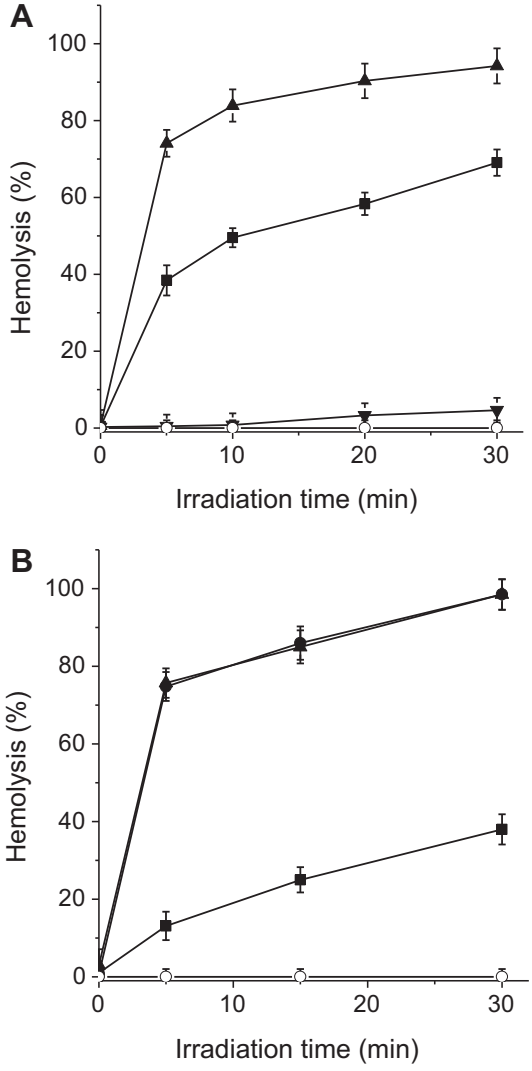

Fig. 4. Photohemolysis of HRB cells ($\sim 10^6$ cells/mL) treated with (A) 5 μM AZnPc (▲), A_4ZnPc (▼) and M4ZnPc (■) and (B) 1 μM (■), 5 μM (●) and 10 μM (▲) AZnPc for 30 min in dark and irradiated with visible light for different times (300 W/m^2) in PBS 0.9% w/v NaCl solution. HRB cells control untreated with photosensitizer and irradiated (○). Values represent mean ± standard deviation of three separate experiments.

a phthalocyanine concentration of 10 μM did not produce significant difference in the HRB photohemolysis in comparison with 5 μM of sensitizer. This behavior may be due to saturation in the amount of intracellular photosensitizer located in the photodynamic action sites. Thus, a further increase in the amount of AZnPc did not produce a greater effect on the cellular damage.

On the other hand, the membrane fragility after photodynamic treatment was compared between AZnPc and M_4ZnPc. Osmotic fragility curves of erythrocytes treated with 5 μM phthalocyanine and irradiated for 3 min with visible light are shown in Fig. 5. This irradiation time was selected to produce a partial damage in the HRB cells. The results indicate that the irradiation of HRB cells in the presence of the photosensitizer produced an increase in the HRB cells osmotic fragility. Thus, the concentration of NaCl corresponding to 50% osmotic hemolysis of native erythrocytes is about 0.43% w/v NaCl, whereas that corresponding to cells treated with AZnPc and M_4ZnPc were 0.70% and 0.64% w/v, respectively. This tendency was previously observed for ZnPc irradiated with various light power [16]. Therefore, these phthalocyanines induced a membrane photodamage, which is evidenced by a diminished in the osmotic resistance. Membrane fluidization may be due to the formation of membrane defects in the HRB cells caused by photochemical oxidation, which plays a significant role in the formation of hemolytic holes [16]. Such impairments of membrane integrity decreased HRB cells osmotic stability.

The morphology of erythrocytes was observed by microscopy after incubation with 5 μM AZnPc and irradiated for 3 min. Representative results are shown in Fig. 6. Microscopic observations showed that the HRB cells changed their normal biconcave discoid shape after photodynamic treatment. Erythrocytes lost their normal profile and presented a spiny configuration with blebs in their surfaces. This effect was present in all studied samples with partial photohemolysis. These results provided evidence about membrane deformation and an increase in the volume of cells indicating a higher fragility after the photodynamic action. Similar deformation of membrane has been previously found in oxidative damage of human erythrocytes [42]. Photosensitized injure of HRB cells produces a significant increase of membrane fluidity due to the formation of defects in HRB cell membrane. This effect decreases erythrocytes osmotic stability and releases the hemoglobin.

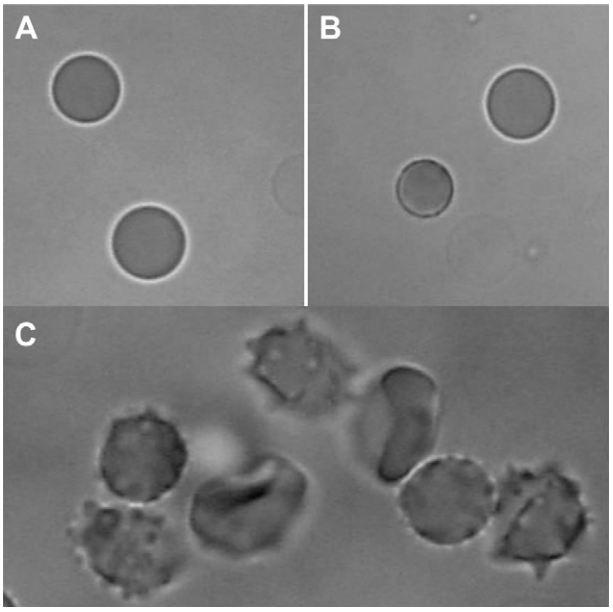

Fig. 6. Photograph showing morphology of HRB cells (A) control untreated with photosensitizer and irradiated for 3 min; (B) control treated with 5 μM AZnPc in dark and (C) treated with 5 μM AZnPc irradiated for 3 min with visible light (300 W/m^2); 100× microscope objective.

In order to elucidate the photodynamic mechanism involved in the photosensitized damage of the HRB membrane, the effect of two suppressors, sodium azide and mannitol, were investigated. Sodium azide is a know quencher of singlet oxygen $O_2(^1\Delta_g)$ preventing type II photoprocess [43]. Thus, HRB cells were incubated with 50 mM azide ion and this concentration was not hemolytic in the dark or under irradiation without phthalocyanine (results not shown). In presence of 5 μM phthalocyanine and light, the addition of azide ion produced a reduction in the photohemolysis of HRB cells (Fig. 7, line 3). After 5 min of irradiation, the hemolysis percentage of erythrocytes was reduced from 75% to 50% for AZnPc,

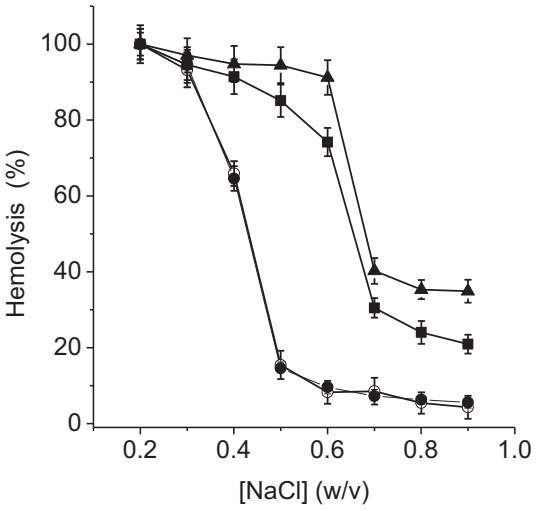

Fig. 5. Osmotic fragility of HRB cells (~10^6 cells/mL) incubated with 5 μM of AZnPc (▲) and M_4ZnPc (■) for 30 min in dark and irradiated 3 min with visible light (300 W/m^2). After irradiation the HRB cells were immediately washed and incubated 30 min in different buffered NaCl solutions. HRB cells control untreated and irradiated (○) and treated with photosensitizer in dark (●). Values represent mean ± standard deviation of three separate experiments.

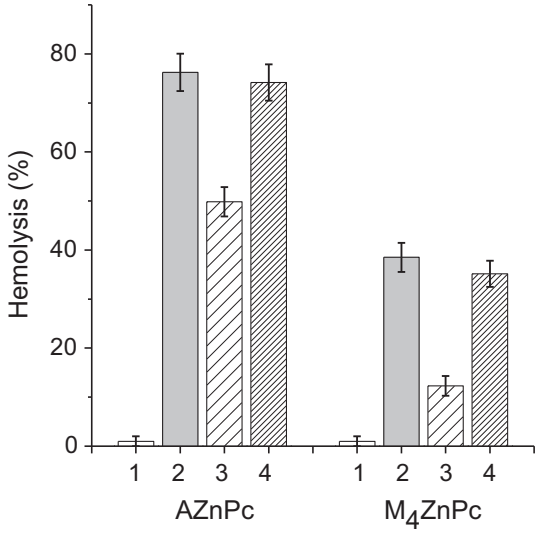

Fig. 7. Influence of azide ion and mannitol on the photohemolysis of HRB cells (~10^6 cells/mL) treated with 5 μM of AZnPc and M_4ZnPc for 30 min in dark in 0.9% w/v NaCl solution; 1) cells control in dark; 2) cells irradiated for 5 min; 3) cells containing 50 mM sodium azide and irradiated for 5 min; 4) cells containing 50 mM mannitol and irradiated for 5 min; visible light (300 W/m^2). Values represent mean ± standard deviation of three separate experiments.

while the hemolysis was reduced from 38% to 12% for M_4ZnPc. Therefore, the azide ion quenched the photocytotoxic species, producing a protective effect on HRB cells.

Otherwise, mannitol was used as a scavenger of the superoxide anion radical and hydroxyl radical [44]. The addition of 50 mM mannitol was not toxic for cells in dark. Also, no hemolytic effect was found for cells irradiated in the presence of mannitol (results not shown). In presence of 5 μM phthalocyanine, photohemolysis percentage was quite similar in the presence or absence of mannitol for both sensitizers after 5 min of irradiation (Fig. 7, line 4). Only a slightly photoprotective effect was observed using M_4ZnPc as photosensitizer.

It has been previously proposed that the damage to erythrocytes cell membrane exerted by photodynamic treatment is due to the formation of reactive oxygen species. Also, it has been shown that this photodynamic activity may be prevented by antioxidants [45]. The present results indicate that photohemolytic efficacy was not significantly affected when mannitol was added to HRB cells sensitized by phthalocyanines. In contrast, the presence of azide ion produced photoprotection of HRB cells by quenching $O_2(^1\Delta_g)$. This suggests that the involvement of $O_2(^1\Delta_g)$ is the main ROS involved in the photohemolysis of HRB cells.

4. Conclusions

In summary, a novel AZnPc phthalocyanine containing an adamantyl group was synthesized by ring expansion reaction of SubPc with phthalonitrile derivative APc. This approach produced selectively asymmetric type A_3B macrocycles. Also, a tetrasubstituted A_4ZnPc was obtained by cyclotetramerization reaction of APc. These phthalocyanines presented similar spectroscopic and photodynamic properties in DMF with high values of $O_2(^1\Delta_g)$ production, where these photosensitizers are mainly dissolved as monomers. However, a higher photodynamic activity was found for AZnPc in a biomimetic system formed by reverse micelles. Also, a higher photohemolytic activity was found for AZnPc in the presence of HRB cells. The efficiency to produce HRB cells hemolysis followed the order: AZnPc $>$ M_4ZnPc $>>$ A_4ZnPc. The photodynamic action induced by AZnPc and M_4ZnPc was accompanied by a decrease in the HRB cells osmotic stability, which lead to the release of hemoglobin. To elucidate the oxidative processes that occur during the hemolysis of HRB cells, the effect of the azide ion and mannitol was analyzed. Photohemolytic efficacy was not affected when mannitol was used as a type I scavenger, in contrast photoprotection was found using sodium azide as $O_2(^1\Delta_g)$ quencher. Thus, photohemolysis mediated by AZnPc occurs mainly by the intermediacy of $O_2(^1\Delta_g)$. Therefore, the presence of an adamantyl unit in the phthalocyanine macrocycle represents an interesting molecular architecture for potential phototherapeutic agents.

Acknowledgments

Authors thank Consejo Nacional de Investigaciones Científicas y Técnicas (CONICET) of Argentina, SECYT Universidad Nacional de Río Cuarto, MINCyT Córdoba and Agencia Nacional de Promoción Científica y Tecnológica (ANPCYT) of Argentina for financial support. M.B.S., T.C.T., M.E.M. and E.N.D. are Scientific Members of CONICET. A.L.O. thanks to CONICET for a doctoral fellowship.

References

[1] S. Luo, E. Zhang, Y. Su, T. Cheng, C. Shi, Biomaterials 32 (2011) 7127–7138.
[2] R.R. Allison, C.H. Sibata, Photodiagn. Photodyn. Ther. 7 (2010) 61–75.
[3] T. Nyokong, Coord. Chem. Rev. 251 (2007) 1707–1722.
[4] P. Matlaba, T. Nyokong, Polyhedron 21 (2002) 2463–2472.
[5] C.G. Claeessens, D. González-Rodríguez, T. Torres, Chem. Rev. 102 (2002) 835–853.
[6] S.M.S. Chauhan, P. Kumari, Tetrahedron 6 (2009) 2518–2524.
[7] T.C. Tempesti, M.G. Alvarez, E.N. Durantini, Dyes Pigm. 9 (2011) 6–12.
[8] A.P. Castano, T.N. Demidova, M.R. Hamblin, Photodiagn. Photodyn. Ther. 1 (2004) 279–293.
[9] P.R. Ogilby, Photochem. Photobiol. Sci. 9 (2010) 1543–1560.
[10] L. Kaestner, A. Juzeniene, J. Moan, Photochem. Photobiol. Sci. 3 (2004) 981–989.
[11] A. Juarranz, A. Villanueva, V. Diaz, L. Rodríguez-Borlado, C. Trigueros, M. Cañete, Anti-Cancer Drugs 4 (1993) 501–504.
[12] I. Rosenthal, V.Y. Shafirovich, N.E. Geacintov, E. Ben-Hur, B. Horowitz, 60 (1994) 215–220.
[13] M. Khalili, L.I. Grossweiner, J. Photochem. Photobiol. B. Biol. 37 (1997) 236–244.
[14] M. Hoebeke, H.J. Schuitmaker, L.E. Jannink, T.M.A.R. Dubbelman, A. Jakobs, A. van de Vorst, Photochem. Photobiol. 66 (1997) 502–508.
[15] A. Marozienė, R. Kliukien&edot, J. Šarlauskas, N. Čėnas, Cancer Lett. 157 (2002) 39–44.
[16] I.B. Zavodnik, L.B. Zavodnik, M.J. Bryszewska, J. Photochem. Photobiol. B. Biol. 67 (2002) 1–10.
[17] L. Kaestner, Gen. Physiol. Biophys. 22 (2003) 455–465.
[18] P.W. Causey, I. Dubovyk, C.C. Leznoff, Can. J. Chem. 84 (2006) 1380–1387.
[19] M.C. García Vior, L.E. Dicelio, J. Awruch, Dyes Pigm. 83 (2009) 375–380.
[20] V.V. Zarubaev, E.L. Golod, P.M. Anfimov, A.A. Shtro, V.V. Saraev, A.S. Gavrilov, A.V. Logvinov, O.I. Kiselev, Bioorg. Med. Chem. 18 (2010) 839–848.
[21] A.A. Kadi, E.S. Al-Abdullah, I.A. Shehata, E.E. Habib, T.M. Ibrahim, A.A. El-Emam, Eur. J. Med. Chem. 45 (2010) 5006–5011.
[22] J. Liu, D. Obando, V. Liao, T. Lifa, R. Codd, Eur. J. Med. Chem. 46 (2011) 1949–1963.
[23] E.I. Yslas, V. Rivarola, E.N. Durantini, Bioorg. Med. Chem. 13 (2005) 39–46.
[24] E.I. Yslas, E.N. Durantini, V.A. Rivarola, Bioorg. Med. Chem. 15 (2007) 4651–4660.
[25] E.I. Yslas, C. Prucca, S. Romanini, E.N. Durantini, M. Bertuzzi, V. Rivarola, Photodiagn. Photodyn. Ther. 6 (2009) 62–70.
[26] I. Scalise, E.N. Durantini, Bioorg. Med. Chem. 13 (2005) 3037–3045.
[27] W. Spiller, H. Kliesch, D. Wöhrle, S. Hackbarth, B. Röder, G. Schnurpfeil, J. Porphyrins Phthalocyanines 2 (1998) 145–158.
[28] T.C. Tempesti, J.C. Stockert, E.N. Durantini, J. Phys. Chem. B. 112 (2008) 15701–15707.
[29] E.A. Dupouy, D. Lazzeri, E.N. Durantini, Photochem. Photobiol. Sci. 3 (2004) 992–998.
[30] A. Ogunsipe, T. Nyokong, J. Mol. Struct. 689 (2004) 89–97.
[31] S. Wei, J. Zhou, D. Huang, X. Wang, B. Zhang, J. Shen, Dyes Pigm. 71 (2006) 61–67.
[32] M.P. Cormick, M. Rovera, E.N. Durantini, J. Photochem. Photobiol. A: Chem. 194 (2008) 220–229.
[33] A. Gomes, E. Fernandes, J.L.F.C. Lima, J. Biochem. Biophys. Methods 65 (2005) 45–80.
[34] M.E. Milanesio, M.G. Alvarez, E.I. Yslas, C.D. Borsarelli, J.J. Silber, V. Rivarola, E.N. Durantini, Photochem. Photobiol. 74 (2001) 14–21.
[35] I. Scalise, E.N. Durantini, J. Photochem. Photobiol. A: Chem. 162 (2004) 105–113.
[36] S.J. Mora, M.P. Cormick, M.E. Milanesio, E.N. Durantini, Dyes Pigm. 87 (2010) 234–240.
[37] C.D. Borsarelli, E.N. Durantini, N.A. García, J. Chem. Soc. Perkin Trans. 2 (1996) 2009–2013.
[38] R.S. Covalcante, H. Imasato, V.S. Bagnato, J.R. Perussi, Laser Phys. Lett. 6 (2009) 64–70.
[39] M.B. Spesia, M. Rovera, E.N. Durantini, Eur. J. Med. Chem. 45 (2010) 2198–2205.
[40] V. Kussovski, V. Mantareva, I. Angelov, P. Orozova, D. Wöhrle, G. Schnurpfeil, E. Borisova, L. Avramov, FEMS Microbiol. Lett. 294 (2009) 133–140.
[41] D. Wöhrle, N. Iskander, G. Graschew, H. Sinn, E.A. Friedrich, W. Maier-Borst, J. Stern, P. Schlag, Photochem. Photobiol. 51 (1990) 351–356.
[42] M. Suwalsky, P. Orellana, M. Avello, F. Villena, FEMS Microbiol. Lett. 45 (2007) 130–135.
[43] M.A. Rubio, D.O. Mártire, S.E. Braslavsky, E.A. Lissi, J. Photochem. Photobiol. A: Chem. 66 (1992) 153–157.
[44] T. Maisch, C. Bosl, R.-M. Szeimies, N. Lehn, C. Abels, Antimicrob. Agents Chemother. 49 (2005) 1542–1552.
[45] A.R. Silva, J.N. Ribeiro, D. Rettori, R.A. Jorge, J. Braz. Chem. Soc. 19 (2008) 1311–1320.